Toward the Comparison of Rare Earth Element and Actinide Behavior in Materials: A Computational Study of Ce- and U-Bearing Britholites

Marjorie Bertolus*

Commissariat à l'Énergie Atomique, Direction de l'énergie nucléaire, DEC/SESC/LLCC, Bâtiment 151, CE Cadarache, 13108 Saint-Paul-lez-Durance, France

Mireille Defranceschi

Commissariat à l'Énergie Atomique, Direction de l'énergie nucléaire; DSOE/RB, Bâtiment 121, CE Saclay, 91191 Gif-sur-Yvette Cedex, France

Received: May 11, 2006; In Final Form: July 25, 2006

We present a computational investigation into the nature of bonds formed by f-elements in materials. The paper presents an example of the incorporation of rare earth elements (REE) and actinides in minerals derived from fluorapatite: $Ca_{10}(PO_4)_6F_2$. These minerals, called britholites, allow many substitutions on all three Ca, P, and F sites and are considered as potential host phases for radioactive elements separated from nuclear waste. REE and actinides have very similar physical and chemical properties, but REE are not radioactive and much more easily handled. REE are, therefore, very often used as a surrogate for actinides in experimental studies. The representative elements of rare earths and actinides chosen for this first investigation are cerium and uranium, respectively. We have studied all the various configurations of $Ca_9X(PO_4)_{6-y}(SiO_4)_yF_2$, where X stands for Ce^{3+}, Ce^{4+}, U^{3+}, and U^{4+}, and *y* is equal to 1 and 2 for three-time and four-time charged cations, respectively. Calculations have been performed within the density functional theory (DFT) framework according to the computation scheme determined in a previous study. The analysis of the energies of the various configurations shows that the incorporation of all the cations considered stabilizes the apatitic structure. This stabilization, however, is greater for four-time charged cations than for three-time charged ones, which shows that Ce and U are both preferentially substituted in the +IV oxidation state. In addition, the substitution in one of the two cationic sites of the apatitic structure is always more favorable. Then, the geometry analysis shows a larger decrease in size of this cationic site for U than for Ce, as well as different volume variations for Ce and U substitutions in the two cationic sites. This cannot be explained by steric effects alone. Finally, the electronic density analysis yields three essential results: U and Ce form significantly covalent bonds, U forms bonds more covalent than Ce, and finally four-time charged cations form more covalent bonds than three-time charged ones. The comparison of these results with the formation enthalpies of the various phases shows a positive correlation between the covalence degree of the bonds formed by the f-element and the stability of the structure. In addition, our results prove that Ce- and U-bearing britholites exhibit very similar energetic, structural, and electronic properties. Ce, therefore, appears to be a good simulant for U.

1. Introduction

Rare earth elements (REE) and actinides have very similar physical and chemical properties, e.g., ionic radii, oxidation states, and coordination numbers in solutions or in materials. This similarity even makes it difficult to separate them when they are simultaneously present in a solution.[1] REE, however, are not radioactive and are more easily handled than actinides. For these reasons, REE are commonly used experimentally as simulants for actinides to mimic both their structural and chemical behavior in solids.[2,3] For instance, neodymium is used as a surrogate for three-time charged minor actinides: americium and curium. Cerium, which exhibits both +III and +IV oxidation states, is used as a simulant for uranium and plutonium when both oxidation states need to be considered. We present here the results of a quantum chemistry investigation of the behavior of REE and actinides in complex materials. This computational study is part of the extensive research performed in our institute on potential host phases for long-life radioactive elements, or radionuclides, separated from French nuclear waste.

We focus on minerals called apatites, which form a very large and abundant family, with the general formula $Me_{10}(XO_4)_6Y_2$, where Me stands for a twice-charged cation, XO_4 for a three-time charged anion, and Y for a −1-charged ion. The most common and simple example of apatite is the fluorapatite: $Ca_{10}(PO_4)_6F_2$. A very interesting and widely exploited property of these minerals is that they allow a large number of substitutions in their structure. Ions with different charges can be substituted in each site provided that the charge balance is maintained, and a large part of the periodic table can be substituted in the apatite structure. In particular, apatites having retained non-negligible quantities of f-elements substituted in their structure for geological times have been found in nature.[4] For this reason, synthetic apatites are studied as potential host phases for radionuclides.

This work is the application of a previous investigation of Nd-bearing apatites.[5] Uranium has been chosen as the first

* To whom correspondence should be addressed. E-mail: marjorie.bertolus@cea.fr.

10.1021/jp0629083 CCC: $33.50
Published on Web 09/02/2006

representative actinide. Unlike other actinides, it has been extensively studied computationally, which will enable us to validate the calculation level chosen. In addition, britholites incorporating the nonradioactive ^{238}U isotope are currently being investigated experimentally. Cerium, its traditional surrogate, has then been chosen as the representative REE.

The first objective of this work is to investigate further the mechanisms of f-element immobilization and determine the nature of bonding in f-element-bearing britholites. Little is known of the atomic-scale mechanisms; even the f-element position in the apatitic structure remains an open question. The second objective is to determine the most stable formulation for a f-element-bearing britholite when there is competition between two possible oxidation states of the f-element. The experimental synthesis of apatites, and in particular substituted ones, is difficult and expensive, so that the knowledge obtained by atomistic modeling can save a lot of time and money in the study of these materials. The third objective is to investigate a possible correlation, which has been brought up for Nd-bearing britholites,[5,6] between the nature of bonding and the material stability. The last objective is the comparison of REE and actinides in these materials. This is important theoretically to determine whether 4f and 5f electrons play equivalent roles in chemical bonding, but it is also important to evaluate how the results of the experiments performed using REE as simulants apply to materials containing real waste.

The outline of this paper is as follows. First, we present the apatitic structure and the radionuclide incorporation in the structure. Then we discuss the computational methods used. Finally, we show the results obtained on the stability, geometries, and electronic structures of the various formulations.

2. Apatites and Incorporation of Radionuclide in the Structure

2.A. Fluorapatite Structure. The apatites[7] studied are derived from fluorapatite, a calcium and phosphate based mineral with formula $Ca_{10}(PO_4)_6F_2$. Fluorapatite crystallizes in the hexagonal structure according to the space group $P6_3/m$.[8] The conventional unit cell, represented on the top of Figure 1, contains 42 atoms corresponding to one $Ca_{10}(PO_4)_6F_2$ formula. The cell parameters are $a = b = 9.398$ Å, and $c = 6.883$ Å. Six equivalent PO_4 groups form the skeleton of the hexagonal structure, which exhibits three different types of sites: two distinct cationic sites containing four and six calcium atoms, respectively, and one anionic site where F atoms are located. The two cationic sites differ by their environments and local symmetries. In site 1, the calcium atom called Ca(1) has nine O atoms as nearest neighbors, the mean interatomic distance between Ca and O being equal to 2.57 Å. This site exhibits C_{3v} symmetry. In site 2, the calcium atom called Ca(2) is surrounded by one F atom and six O atoms of three distinct types. The mean interatomic distance between Ca(2) and its nearest neighbors is 2.41 Å. Site 1 thus has a substantially larger volume than site 2. Finally, F are located in tunnels formed by Ca(2).

TABLE 1: Examples of Cations with Various Oxidation States Which Can Be Substituted to Ca in the Fluorapatite Structure

oxidation state	cation
+I	Na, K
+II	Sr, Ba, Cd, Pb
+III	Al, La, Nd, Ce
+IV	Ce, Th, U

The fluorapatite accepts many substitutions on each of the three Ca, PO_4, and F sites. Examples of ions that can be substituted in the Ca sites of the fluorapatite structure are listed in Table 1. These substitutions can be of various types. They can be simple, where only one ion is substituted, or multiple when several ions are exchanged simultaneously. Particular cases of multiple substitutions are compensated substitutions, where two ions are replaced with ions with different charges so as to maintain charge balance in the structure. Finally, these substitutions can be total, i.e., the initial ions are completely

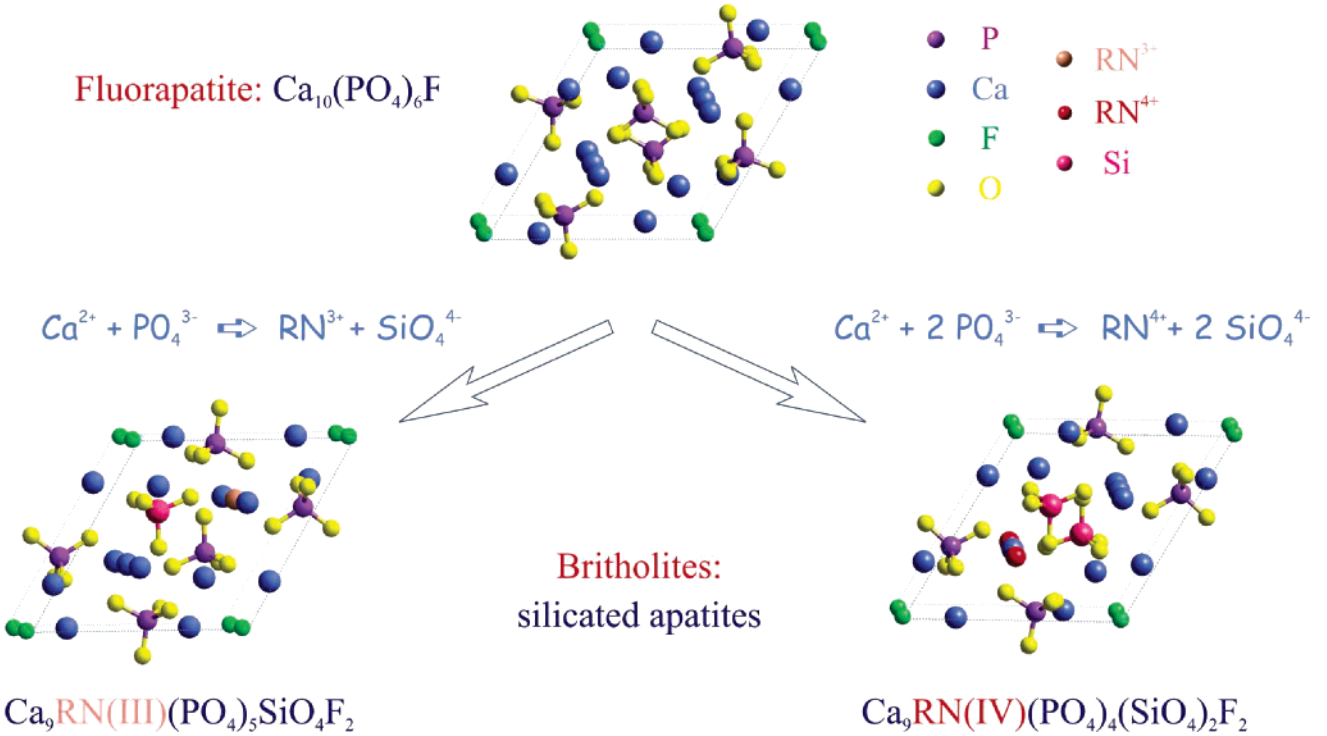

Figure 1. Conventional cell of fluorapatite and substitutions necessary to maintain electroneutrality after the substitution of one Ca^{2+} cation by a three- or four-time charged f-element.

substituted, or partial where only a fraction of the initial ion is replaced. Natural apatites have been shown to have a good propensity to accommodate nonstoichiometry.

2.B. Incorporation of One Three- or Four-Time Charged Cation. The apatitic structure can incorporate many REE and actinides on the Ca site. Because these elements are mostly in the +III or +IV oxidation state, there need to be charge compensation on one of the other sites. In the case of the substitution of one Ca^{2+} cation by a three-time charged f-element X, two ways can be considered to maintain electroneutrality. One can either replace another Ca by a simply charged cation, for instance Na^+, to obtain the apatite with formula $Ca_8NaX(PO_4)_6F_2$, or one four-time charged anionic group (e.g., one silicate SiO_4^{4-}) can be substituted to one of the phosphate PO_4^{3-} group, which yields the $Ca_9X(PO_4)_5SiO_4F_2$ formula. Such a silicated apatite is called britholite. It has been shown computationally on Nd-bearing systems that the second way yields the most stable material by far. Furthermore, from the application point of view, apatites with one or two silicate groups have been shown to be more resistant to radioactive decay than totally phosphated ones.[9] For these reasons, we focus on britholites in our investigation, and the silicate substitution is the only way considered for f-element incorporation. A tetravalent f-element-bearing britholite with formula $Ca_9X(PO_4)_4(SiO_4)_2F_2$ is, therefore, obtained in replacing two phosphate groups by two silicate groups. The SiO_4 substitutions necessary to maintain electroneutrality after the introduction of one three- or four-time charged cation are shown in Figure 1. One important consequence of substitutions, and in particular of compensated substitutions, is that initially equivalent sites become nonequivalent so that structures lose their hexagonal symmetry. This gives rise to a large number of distinct configurations for each composition. A three-time charged cation can be substituted in site 1 or site 2, and SiO_4 can replace any of the six phosphate groups, yielding twelve different configurations. A four-time charged cation can again be substituted in site 1 or site 2, and the two SiO_4 groups can replace any of the six phosphate groups. This gives rise to 30 different configurations.

There is, however, no a priori idea as to which configuration is the most stable from the experimental point of view.[5,10] The phenomena governing cation position in the structure are still uncertain. Furthermore, the silicate position has always been considered as a second-order effect and has never been investigated experimentally. Finally, experimental techniques for structure determination, such as X-ray diffraction or EXAFS, provide only average values for materials that are difficult to synthesize in a pure and homogeneous state. The computational study on Nd-bearing apatites[5] has shown first indices toward the relevant role of covalent bonding in stability. Moreover, it has shown that the most stable configurations of the Nd-britholite exhibit the shortest Nd−Si distances, but it remains to be confirmed that this still holds true for Ce and U, especially in the +IV oxidation state. We have, therefore, considered in this study all the possible configurations for the various formulations.

3. Computational Details

3.A. Choice of Method. The systems studied and the properties to be determined exhibit a certain number of specificities, which have to be taken into consideration for the choice of computation method. On the one hand, the compositions studied include heavy elements, which are delicate to study theoretically. First, relativistic effects are significant and cannot be neglected. Then, there are very few model potentials for REE and actinides in solid phase, and we are interested in the nature of bonding in our materials. We have, therefore, chosen to use a first-principles method, which does not need a prior knowledge of the system and considers electrons explicitly. Furthermore, these methods enable us to describe the different types of bonds present in the system, including covalent, with the same accuracy. On the other hand, the systems considered make calculations long and difficult. Apatites exhibit large unit cells as well as very low symmetry, especially after f-element incorporation. A large number of different configurations thus need to be considered. We have, therefore, chosen to use the density functional theory (DFT), which allows the introduction of electronic correlation at a relatively low cost. Furthermore, we have decided to work in the pseudopotential approach, which enables us to consider only valence electrons, reducing further the computation cost, especially for f-elements.

There are few ab initio studies concerning complex actinide-bearing solids. The accuracy of the results is, therefore, difficult to assess, especially as far as the energies are concerned. The comparison of computational investigations using DFT, and in particular the generalized gradient approximation and ultrasoft pseudopotentials[11,12] with experimental results, however, shows that this calculation level yields very good results for geometries. Moreover, the previous study on Nd-bearing apatites[5] has shown that the accuracy on binding energies is slightly larger than 1% and much better on relative energies of similar configurations. Energy differences of 0.1 eV or even 0.05 eV should, therefore, be meaningful.

3.C. Density Functional Theory Implementation. We have used the computation scheme determined in the study of Nd-bearing apatites.[5] This scheme, which has been shown to yield a good accuracy on the structural and energetic properties of f-element-bearing apatites in reasonable computation times, consists of two steps.

First, geometry optimizations and total energy calculations are performed using the commercial version of the Cambridge serial total energy package program (CASTEP).[13−15] In this code, periodic boundary conditions are used, and the occupied electronic orbitals are expanded in a plane wave basis. The expansion includes all plane waves with kinetic energies less than a cutoff energy E_{cut}, chosen to ensure convergence with respect to the basis set. Finite basis corrections are evaluated numerically based on the method introduced by Francis and Payne using the total energy calculated at three different values of the kinetic energy cutoff.[16] The Brillouin zone is sampled with the Monkhorst−Pack scheme[17] so that distances between sampling points are always less than 0.05 $Å^{-1}$. The pseudopotential approximation is used: only the valence electrons are represented explicitly in the calculations, the core states and valence−core interactions being described by nonlocal pseudopotentials. Core states are described using small-core ultrasoft pseudopotentials[18] built in CASTEP. These pseudopotentials have been fitted to all electrons results yielded by the Koelling−Harmon equation[19] and, therefore, include scalar relativistic effects. They have been validated for Ce and U on various compounds.[11] A 370 eV energy cutoff is used in the plane wave basis expansion. Exchange and correlation effects have been calculated in the generalized gradient approximation (GGA) using the Perdew−Wang parametrization.[20] A 42-atom cell is considered, and symmetry is used whenever possible. Calculations are performed using spin-polarization but neglecting zero-point effects. These effects would be very time-consuming to estimate, and we consider that the atoms involved in our materials are heavy enough to justify this approximation.

Geometry optimizations consist of simultaneous optimization of cell parameters and of internal coordinates.

Second, total energy calculations and charge density analyses are performed at the CASTEP equilibrium geometry using the solid module of the commercial version of the DMol^3 program.[21,22] Dmol^3 uses a basis set of numeric atomic functions that are exact solutions to the Kohn−Sham equations for the atoms. In our study, a double numeric-polarized (DNP) basis set equivalent to a polarized valence basis set 6-31G* is used. These basis sets have been designed to minimize basis set superposition effects,[23] which have therefore been neglected. The same functional is used as for the geometry optimizations in CASTEP. Spin-polarized calculations are also performed. Atomic energies are computed through the exact DFT calculations on spherically symmetric grids, which are used to determine the basis sets. Binding energies (E_b) are calculated from the total energy (E_t) according to the formula as follows:

$$E_b(\text{material}) = -E_t + \sum_{\text{atoms}} n_{\text{atom}} E(\text{atom}) \quad (1)$$

According to this definition, E_b is positive when the material is stable. Formation enthalpies at 298 K are then computed from the DFT binding energies and the atomic enthalpies at 298 K using the formula as follows:

$$\Delta H_f^{298K}(\text{material}) = -E_b + \sum_{\text{atoms}} n_{\text{atom}} \Delta H_f^{298K}(\text{atom}) \quad (2)$$

These formation enthalpies are necessary to compare materials with different formulas. The ΔH_f^{298K}(atom) values used for the formation enthalpy estimations have been taken from ref 24.

For charge density analysis, we have chosen to perform population analyses using the Mulliken scheme. Care should always be exercised when interpreting the results of population analyses because the assignment of electronic charge to individual atoms in a solid is not a unique procedure, and the Mulliken scheme is a simplistic method. However, we have compared results of calculations performed using the same basis set at the same level of theory as well as atoms in a similar environment. Moreover, we have considered only charge differences and never the absolute values obtained to ensure independence from the arbitrary character of this scheme. Because this method is fast, we have performed Mulliken population analyses on all the configurations studied, which has enabled us to take meaningful statistics. In addition, we have computed deformation density maps. The deformation density is the difference between the valence electronic density in a material and the sum of the valence densities of the various atoms involved. Isodensity plots in different planes of the unit cell can then be calculated and represented as maps. These maps enable one to see the variations in the charge density corresponding to bonding. The analysis of the deformation density is much more precise than that of the total electronic density because the latter exhibits large fluctuations in a material, which often hides the fine variations involved by bond formation. Moreover, the use of deformation density cancels out the pseudopotential effects. We think that the combination of these two methods of charge density analysis is reliable enough for our purpose and can provide helpful information regarding charge transfers occurring in the structure.

4. Results

We have determined the equilibrium geometry, the formation enthalpy, as well as performed the charge density analysis on the 12 different configurations for Ce^{3+}- and U^{3+}-bearing britholites and on the 30 configurations for Ce^{4+}- and U^{4+}-bearing ones. We will discuss the results obtained according to three aspects: energetic, geometries, and electronic densities. For each comparison in the next paragraphs, the results given are the results obtained for the most stable configuration relative to the SiO_4 position.

TABLE 2: Binding Energy in eV and ΔH_f^{298K} in kJ/mol of Fluorapatite and of the Most Stable Configurations of Ce- and U-Britholites with f-Element in Site 1 or Site 2

	E_b (eV)	ΔH_f^{298K} (kJ/mol)
Fluorapatite	247.62	−14075.4
Ce^{3+}-britholite 1	252.38	−14156.7
Ce^{3+}-britholite 2	252.43	−14161.2
U^{3+}-britholite 1	254.23	−14218.3
U^{3+}-britholite 2	254.16	−14224.9
Ce^{4+}-britholite 1	253.74	−14154.3
Ce^{4+}-britholite 2	253.99	−14178.7
U^{4+}-britholite 1	257.07	−14365.5
U^{4+}-britholite 2	257.24	−14381.6

TABLE 3: Cell Parameters in Å and Cell Volume in Å^3 of the Most Stable Configurations of Ce- and U-Britholites with f-element in Site 1 or Site 2

	a	*b*	*c*	*V*
Fluorapatite	9.452	9.452	6.883	532.525
Ce^{3+}-britholite 1	9.444	9.465	6.910	536.029
Ce^{3+}-britholite 2	9.431	9.493	6.888	534.743
U^{3+}-britholite 1	9.477	9.485	6.921	539.611
U^{3+}-britholite 2	9.456	9.506	6.900	538.743
Ce^{4+}-britholite 1	9.460	9.489	6.873	533.640
Ce^{4+}-britholite 2	9.465	9.486	6.839	531.870
U^{4+}-britholite 1	9.534	9.523	6.896	539.177
U^{4+}-britholite 2	9.446	9.464	6.866	532.133

4.A. Energetic. The binding energies and formation enthalpies of fluorapatite and of the most stable configurations of the substituted britholites are listed in Table 2. The energetic order from the most stable to the least stable formulation is as follows: U^{4+}-, U^{3+}-, Ce^{4+}-, Ce^{3+}-bearing britholite, and then fluorapatite. The analysis of these enthalpies shows that the incorporation of all the cations considered stabilizes the apatitic structure. This stabilization, however, is larger for the four-time charged cations than for the three-time charged ones, which shows that Ce and U are both preferentially substituted in the +IV oxidation state. Then, U-bearing britholites are more stable than Ce-bearing ones. In addition, the substitution in the second cationic site located next to one F atom is always more favorable. The energy differences between the configurations with the f-element in site 1 or site 2, however, are small. Finally, the relative stabilities are the same for the Ce and U. The most stable configurations relative to the f-element and SiO_4 positions are the same for Ce and U for both +III and +IV oxidation states. However, all the energy differences between the different configurations and formulations are larger for U than for Ce.

4.B. Geometries. We have first analyzed the cell parameters and volumes obtained for the various f-element-bearing britholites. They are listed in Table 3 for the most stable configurations of substituted britholite with the f-element in site 1 or site 2. Relatively large volume variations compared to the fluorapatite can be observed. Then, the unit cell volume decreases for f-element substitution in site 2, while it increases for substitution in site 1. Furthermore, for the most stable configurations, the unit cell volume increases in the case of three-time charged f-element insertion, while it decreases for four-time charged f-element insertion. Finally, the most stable structure for each britholite formulation exhibits the smallest cell. Table

TABLE 4: Ionic Radii in Å of the Various Cations Considered for Two Different Coordination Numbers

	Ca	Ce^{3+}	Ce^{4+}	U^{3+}	U^{4+}
6-time coordinated	1.14	1.15	1.01	1.165	1.03
8-time coordinated	1.26	1.283	1.11	-	1.14

TABLE 5: Site Sizes, i.e., Average Distances between a Cation and its First Neighbors, in Å, for the Various Cations for the Fluorapatite, as Well as for the Most Stable Configurations of Ce- and U-Bearing Britholites

cation/site	1	2
Ca^{2+}	2.570	2.413
Ce^{3+}	2.549	2.456
Ce^{4+}	2.461	2.361
U^{3+}	2.550	2.460
U^{4+}	2.458	2.360

4 lists the effective ionic radii[25] for the various cations considered. It can be seen that Ce^{4+} is slightly smaller than U^{4+}, which is smaller than Ca^{2+}, which is smaller than Ce^{3+}, which is in turn slightly smaller than U^{3+}. The cell volumes observed for the most stable configurations are, therefore, consistent with the ionic radii. The difference between site 1 and site 2, however, is not.

Second, we have looked into a geometrical origin to the stability of the structures. The analysis of the structures for all the configurations of the Ce^{3+}- and U^{3+}-bearing britholites obtained shows that the most stable structures exhibit the shortest f-element−Si distances, as was the case for Nd-bearing britholite. Moreover, the same configurations are the most stable for the three f-elements. In the case of the substitution of a four-time charged cation, the situation is not as clear-cut. The lowest energy configurations with f-elements in site 1 exhibit two very short f-elements−Si bonds. In the case of the substitution in site 2, the most stable configurations exhibit one very short bond and a longer one. Ce and U are in all cases located next to both SiO_4 groups. Local charge balance in the material is therefore favorable. This enables us to predict which structures are likely to be the most stable and will limit the number of structures to investigate in further studies. This will reduce significantly the computation time, especially in the case of the insertion of a four-time charged f-element.

Finally, we have analyzed the size of the cationic sites around the substituted atoms, i.e., the average distance between a cation and its first neighbors. Table 5 lists the site sizes calculated for the five cations Ca^{2+}, Ce^{3+}, Ce^{4+}, U^{3+}, and U^{4+} in the fluorapatite structure as well as in the most stable configurations of f-element-bearing britholites. The first cationic site is smaller for Ce and U in both +III and +IV oxidation states than for Ca. On the contrary, the second cationic site is greater for the three-time charged f-elements than for Ca, while they are smaller for the four-time charged ones. As seen in the previous paragraph, the ionic radii order is as follows: $Ce^{4+} < U^{4+} < Ca^{2+} < Ce^{3+} < U^{3+}$. These ionic radii explain why Ce^{4+} and U^{4+} substitute in site 2, which is the smaller cationic site. Steric considerations also explain the decrease in site size after Ce^{4+} and U^{4+} substitution in site 1 and 2. Ionic radii are not consistent, however, with the decrease in size after Ce^{3+} and U^{3+} substitution in site 1, or the difference between Ce^{3+} and U^{3+} substitution in site 1 and 2. They cannot explain either why Ce^{3+} and U^{3+} substitute in site 2, which is the smaller cationic site, or why the cationic sites are slightly smaller for U than for Ce. This could be an effect of the electronic structure and could in particular mean that the bonds formed by Ce and U are not purely ionic.

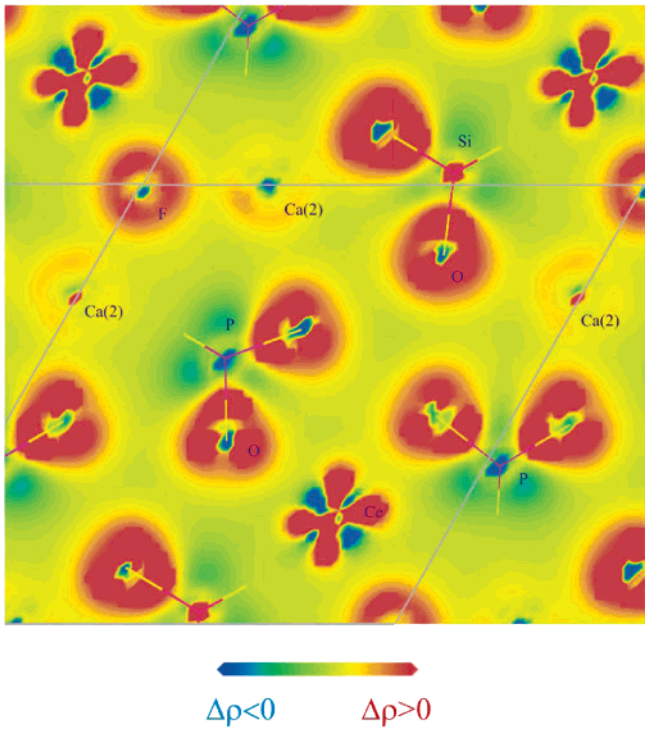

Figure 2. Charge deformation map in the (001) plane of the most stable configuration of the Ce^{3+}-bearing britholite.

4.C. Analysis of Electronic Density. To get further insight into the nature of bonding in our system, we have first analyzed the electronic density using density deformation maps. The deformation density is the difference between the valence electronic density in a material and the sum of the valence densities of the various atoms involved. Zones of positive deformation density, therefore, correspond to zones where atoms have gained electronic density in the crystal compared to the atomic state. On the contrary, zones of negative deformation density show electronic density loss. Moreover, the localization of these zones between two atoms gives insight on the nature of bonds between them. In the case of ionic bonds, the deformation density is symmetric and spherical around the ion core, and is only slightly distorted by the other atoms of the crystal. In the case of a covalent bond, this deformation density is no longer spherical, but strongly distorted toward the atoms with which bonds are formed. One characteristic feature of this directional bonding on maps is the presence of "lobes" exhibiting different densities around the atom.

We have represented in Figure 2 the deformation density map in the (001) plane for the most stable configuration of the Ce^{3+}-britholite. The PO_4 tetrahedra can be seen clearly on this figure. Positive deformation is localized on O atoms, while negative deformation is localized on P atoms, as expected from the electronegativities of both atoms. The deformation densities on O and P are both very distorted. Three distinct lobes in the (001) plane can be seen on O, one dark one toward P, and two slightly weaker ones toward the neighboring Ca atoms. Three lobes pointing between the O atoms are also observed for P. This shows the directional bonding and the strong covalent character of the PO_4 groups, which form the skeleton of the fluorapatite. It can be observed that the Si−O bond is slightly more ionic than P−O. The density on Si is more spherical, and the lobes on O and Si are less clearly defined. This is consistent with the electronegativities of P and Si. It can also be seen that the density around Ca atoms is spherical, with a much smaller deformation intensity. Moreover, no difference can be seen between Ca atoms

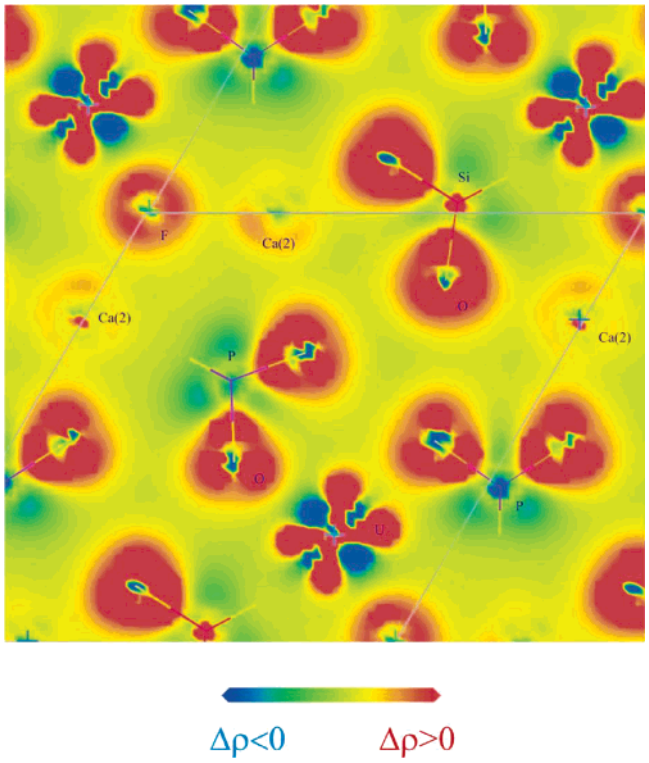

Figure 3. Charge deformation map in the (001) plane of the most stable configuration of the U^{4+}-bearing britholite.

in site 1 (not represented here) and site 2 despite their different environments. Similarly, the density around the F atoms next to Ca atoms is little distorted. The symmetry of the deformation is spherical, with three weak lobes toward the Ca atoms. This is characteristic of ionic character and shows that Ca and F form, as expected, mostly ionic bonds. On the contrary, density on Ce atoms is very different from the density on Ca atoms. The deformation density on Ce atoms extends far away from the ionic core and is far from spherical. It exhibits an alternation of positive and negative lobes, the negative lobes pointing toward the positive lobes of O or F atoms. Moreover, the opposite lobe on O and F is larger and more intense in color than in fluorapatite. This shows a significant covalent character of the Ce−O and Ce−F bonds. Ce^{4+} exhibits the same behavior as Ce^{3+}, the atomic lobes on Ce^{4+} being slightly larger. That would indicate a slightly more covalent bonding.

We have finally represented in Figure 3 the deformation density map in the (001) plane of the U^{4+}-britholite. The deformation density is very similar to the density in the Ce^{3+}-britholite. The lobes around the U atom extend even further spatially than in the Ce case, and a more intense lobe toward U can be observed on O and F atoms. This also shows the significant covalent character of the U−O and U−F bonds. U^{3+} exhibits the same behavior as U^{4+}. The atomic lobes on U^{3+}, however, are slightly smaller.

To refine these qualitative observations we have computed partial charges using the Mulliken method. First, the Mulliken charges on Si and O bonded to Si are larger than charges on P and O bonded to P. This confirms than Si−O bonds are more ionic than P−O bonds. Moreover, Table 6 shows the average charge decrease (in %) between the formal charge and the Mulliken charges for the five cations considered in the various formulations. It is observed that the charges on f-elements are considerably less than the formal +3 or +4 charges, while charges on Ca atoms are close to +2. The trends are similar for Ce and U; in particular, charge decrease is stronger for four-time charged cations than for three-time charged ones. The average charge decrease, however, is stronger for U than for Ce. These observations are consistent with the cationic site size observed. In addition, we present in Table 7 the charge decrease (in %) on the neighbors of the various f-elements. A significant charge decrease is observed in all configurations on f-element nearest neighbors compared to Ca nearest neighbors, especially on the F atoms.

TABLE 6: Charge Decrease (in %) between Formal and Mulliken Charges of Cations in Fluorapatite, Ce- and U-Bearing Britholites

cation/site	1	2
Ca	23	22
Ce^{3+}	53	47
Ce^{4+}	60	56
U^{3+}	62	56
U^{4+}	68	63

TABLE 7: Charge Decrease (in %) on f-Element Neighbors in Fluorapatite, Ce- and U-Bearing Britholites

cation/site	O site 1	O site 2	F site 2
Ce^{3+}	3	3	7
Ce^{4+}	5	6	11
U^{3+}	6	7	12
U^{4+}	8	10	18

The combination of the low charges on Ce and U atoms and on their neighbors shows that they form significantly covalent bonds in britholites, as was seen on the deformation density maps. The covalence is slightly larger for four-time charged cations than for three-time charges ones, and for U than for Ce. This stronger covalent character of the bond formed by actinides than by REE has already been observed in solutions.[26] Finally, if we compare the partial charges and the formation enthalpies of the various phases discussed in the energetic section, we see that there is a positive correlation between the degree of covalency of the bond formed by the f-element and the stability of the structure. This confirms the first results obtained on the Nd-bearing britholites.

5. Conclusion

In the present study, we have shown that the various Ce- and U-bearing britholites are more stable than fluorapatite. The Ce and U incorporation stabilizes the structure when it is balanced by the incorporation of one or two SiO_4 groups. This stabilization, however, is larger for the four-time charged cations than for the three-time charged ones, which shows that Ce and U are both preferentially substituted in the +IV oxidation state. Furthermore, these results show that U-bearing britholites are more stable than Ce-bearing ones. Then, for the structures, it is found that the various f-elements substitute preferably in the second cationic site. Moreover, the most stable structures exhibit the shortest f-element−Si distances. Local charge balance therefore seems favorable. Then, concerning the electronic structure, we have shown that Ce and U exhibit similar bonding in britholites and form significantly covalent bonds. U forms bonds more covalent than those of Ce, which is consistent with the behavior of REE and actinide cations in solution. In addition, the comparison between the partial charges and the formation enthalpies of the various phases shows the positive correlation between the degree of covalence of the bonds formed by the f-element and the stability of the structure. Finally, Ce- and U-bearing britholites exhibit similar energetic, structural, and electronic properties. Ce, therefore, seems to be a good simulant for U.

References and Notes

(1) Nash, K. L. In *Handbook on the Physics and Chemistry of Rare Earths*; Gschneider, K. A., Eyring, L., Choppin, G. R., Lander, G. H., Eds.; North-Holland: Amsterdam, 1994; Vol. 18, p 197.

(2) Ramsey, W. G.; Bibler, N. E.; Meaker, T. E. *Waste Management 95*, WM Symposia, 1995; Record 23828.

(3) Guy, C.; Audubert, F.; Lartigue, J.-E.; Latrille, C.; Advocat, T.; Fillet, C. *C. R. Phys.* **2002**, *3*, 827.

(4) Bros, R.; Carpena, J.; Sere, V.; Beltritti, A. *Radiochim. Acta* **1996**, *74*, 277.

(5) Bertolus, M.; Defranceschi, M. *Int. J. Quantum Chem*. **2006**, to be published.

(6) Louis-Achille, V.; Defranceschi, M. *Vide* **1998**, *287*, 224.

(7) Elliott, J. C. *Structure and Chemistry of the Apatites and Other Calcium Orthophosphates, Studies in Inorganic Chemistry*; Elsevier: New York, 1994.

(8) Hugues, J. M.; Cameron, M.; Crowly, K. D. *Am. Mineral*. **1989**, *74*, 870.

(9) Boyer, L.; Ph.D. Dissertation, Institut National Polytechnique de Toulouse, 1998.

(10) Elliott, J. C. *Structure and Chemistry of the Apatites and Other Calcium Orthophosphates, Studies in Inorganic Chemistry*; Elsevier: New York, 1994; pp 82−94.

(11) Pickard, C. J.; Winkler, B.; Chen, R. K.; Payne, M. C.; Lee, M. H.; Lin, J. S.; White, J. A.; Milman, V.; Vanderbilt, D. *Phys. Rev. Lett.* **2000**, *85*, 5122.

(12) Milman, V.; Winkler, B.; White, J. A.; Pickard, C. J.; Payne, M. C.; Akhmatskaya, E. V.; Nobes, R. H. *Int. J. Quantum Chem.* **2000**, *77*, 895.

(13) *Castep* version 4.2.1; Accelrys Inc.: San Diego, CA, 2000.

(14) Payne, M. C.; Teter, M. P.; Allan, D. C.; Arias, T. A.; Joannopoulos, J. D. *Rev. Mod. Phys.* **1992**, *64*, 1045.

(15) Segall, M. D.; Lindan, P. L. D.; Probert, M. J.; Pickard, C. J.; Hasnip, P. J.; Clark, S. J.; Payne, M. C. *J. Phys.: Condens. Matt.* **2002**, *14*, 2717.

(16) Francis, G. P.; Payne, M. C. *J. Phys.: Condens. Matter* **1990**, *2*, 4395.

(17) Monkhorst, H. J.; Pack, J. D. *Phys. Rev. B* **1976**, *13*, 5188.

(18) Vanderbilt, D. *Phys. Rev. B* **1990**, *41*, 7892.

(19) Koelling, D. D.; Harmon, B. N. *J. Phys. C: Solid State Phys*. **1977**, *10*, 3107

(20) Perdew, J. P.; Wang, Y. *Phys. Rev. B* **1992**, *45*, 13244.

(21) Delley, B. *J. Chem. Phys*. **1990**, *92*, 508.

(22) Delley, B. *J. Chem. Phys*. **2000**, *113*, 7756.

(23) Delley, B. *J. Chem. Phys*. **1990**, *92*, 508.

(24) Cox, J. D.; Wagman, D. D.; Medvedev, V. A. *CODATA Key Values for Thermodynamics*; Hemisphere: New York. 1989.

(25) WebElements. http://www.webelements.com; Winter, M., Ed.; The University of Sheffield and WebElements Ltd, U.K.; 1993.

(26) Guillaumont, D. *J. Phys. Chem. A* **2004**, *108*, 6893.